Ships and Offshore Structures
Publication details, including instructions for authors and subscription information:
http://www.tandfonline.com/loi/tsos20

Equivalent shell element for ship structural design

Eero Avi[a], Ingrit Lillemäe[b], Jani Romanoff[b] & Ari Niemelä[a]
[a] STX Finland, Telakkakatu 1, Turku, Finland
[b] Department of Applied Mechanics, Marine Technology, Aalto University, Aalto, Finland
Published online: 06 Aug 2013.

To cite this article: Eero Avi, Ingrit Lillemäe, Jani Romanoff & Ari Niemelä (2015) Equivalent shell element for ship structural design, Ships and Offshore Structures, 10:3, 239-255, DOI: 10.1080/17445302.2013.819689

To link to this article: http://dx.doi.org/10.1080/17445302.2013.819689

Ships and Offshore Structures, 2015
Vol. 10, No. 3, 239–255, http://dx.doi.org/10.1080/17445302.2013.819689

Equivalent shell element for ship structural design

Eero Avi[a*], Ingrit Lillemäe[b], Jani Romanoff[b] and Ari Niemelä[a]

[a]*STX Finland, Telakkakatu 1, Turku, Finland;* [b]*Department of Applied Mechanics, Marine Technology, Aalto University, Aalto, Finland*

(*Received 28 March 2013; final version received 24 June 2013*)

This paper presents an equivalent shell element for assessing the ship global and local static and vibration response in early design phases. The element provides a computationally economic tool for global analysis and the same mesh can be used in primary, secondary and tertiary level. The stiffened panel is considered as a three layer laminate element, where the first layer represents the plate, the second layer represents the stiffener web and the third layer represents the stiffener flange. The layers are described as 2D iso- and orthotropic materials, where elasticity matrices are found by applying the rule of mixtures. The element includes the in-plane, membrane-bending coupling, bending and additionally also shear stiffness, which follows the Reissner-Mindlin plate theory for anisotropic homogenous shells. The local plate bending response between the stiffeners is considered as well. The developed shell formulation has been implemented in commercial FE software FEMAP with NX Nastran and demonstrated through two case studies. Results are validated against 3D fine mesh quasi-static and vibration analyses and very good agreement is observed.

Keywords: passenger ship; equivalent laminate element; conceptual structural design; quasi-static analysis; vibration analysis

Nomenclature

List of symbols

A	area
ABD	in-plane (A), membrane-bending coupling (B) and bending (D) stiffness
B, b	breadth
D_Q	shear stiffness
E	Young's modulus
G	shear modulus
H	height
h	stiffened panel height
I	second moment of area
k	shear correction factor
L	length
le	mesh size
M	bending moment
N	normal force
Q	shear force
q	pressure load
s	stiffener spacing
t	thickness
u, v, w	displacements in x-, y- and z-directions
x, y, z	coordinates
γ	shear strain
ε	normal strain
θ	rotation
κ	curvature
ν	Poisson's ratio
σ	normal stress
τ	shear stress

List of sub- and superscripts

0	reference to mid-plane of panel
avg	average
b	bottom
f	stiffener flange
g	global
i	index
l	local
na	neutral axis
p	plate
Q	shear force
s	steel
t	top
tot	total
w	stiffener web
x, y, z	coordinates

1. Introduction

In the design of modern passenger ships, new and challenging concepts are utilised, which means that advanced numerical methods are needed to accurately evaluate global, i.e. primary, and local, i.e. secondary and tertiary responses (Gudmunsen 2000). Generally two types of global response analysis are performed: equivalent quasi-static and vibration. In the static analysis, the stresses and deformations of the hull girder due to hogging, sagging, racking, torsion and docking load conditions are obtained (DNV 2013, 2007).

*Corresponding author. Email: eero.avi@stxeurope.com

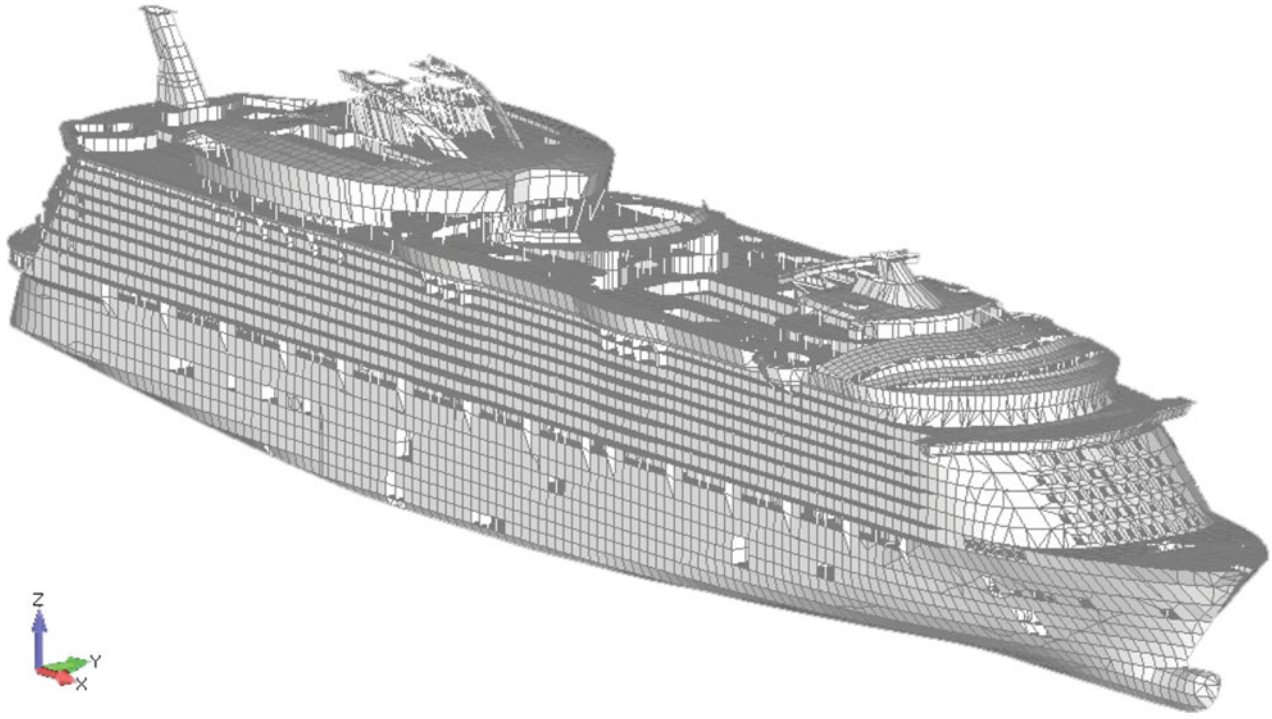

Figure 1. Global FE model of a cruise ship. (This figure is available in colour online.)

If large lateral loads occur, the examination of the local structures becomes essential as well. Vibration response analysis is especially important for cruise ships, where vibration limits are commonly determined from the passenger comfort and machinery lifetime requirements. The standard procedure for preventing undesired vibrations is to obtain the natural frequencies of the ship structures correctly and restrain them above the allowable resonant limit (Okumoto et al. 2009). A complete vibration analysis of a ship does not only include global vibration modes but also an examination of local structures, such as cabin areas, restaurants, engine rooms, etc.

Nowadays, fine mesh finite element analysis (FEA) is regarded as the most reliable method for evaluating the cruise ship structural behaviour (Paulling 1968; Hughes et al. 1980; McVee 1980; Fransman 1988; Heder and Ulfvarson 1991; ISSC 1997; Naar 2006; DNV 2007; Jang et al. 2008; Andric and Zanic 2010; Kurki 2010; Romanoff et al. 2011). However, this method is computationally very expensive. Creation of the global cruise ship model can take few months and calculation can take some additional weeks. Hence, fine mesh FEA is unsuitable for cruise ships in initial design phases, where the analysis has to be performed relatively quickly and several large changes must be possible as the general arrangement changes.

Coarse mesh global FE analysis is the most convenient way to obtain the response of the complete vessel. The ship global FE model (Figure 1) is created so that the secondary stiffeners are incorporated into the plate or shell element formulation in a way that it results in equivalent stiffness, bending and vibration response (DNV 2007). The primary stiffeners such as girders and web frames are explicitly modelled due to their large participation in overall stiffness of the structure. They are usually discretised with offset beam elements according to Timoshenko theory and their length is identical to the size of the neighbouring equivalent plate element.

Most common way to represent the equivalent plate element is by lumping the stiffeners (Hughes 1988). In the lumping process, all secondary stiffeners are *put* inside of the topological beam elements, which are located at the edges of the plate element. Each stiffener causes an increase in the cross sectional properties of the lumped beam elements. Lumping is one of the simplest approaches but it is also less accurate. For more precise analysis, Hughes (1988) suggested the orthotropic plate technique, where the stiffeners are blended with the plating so that the plate has different stress-strain properties in two directions. Since the stiffened panel is represented as one orthotropic plate, this approach does not allow analysing plate and stiffener separately and the obtained normal stress is average of the plate and the stiffener. For more advanced analysis, Hughes (1988) proposed a separate 'stiffener element', where the stiffeners are described as a special membrane element, which extends over the same area as the plating and has the same corner nodes and degrees of freedom (DOF). The

stiffness matrix of the complete stiffened panel is obtained by summing the stiffness matrices of the plate and the 'stiffener element'. All the equivalent element techniques proposed by Hughes can only represent the in-plane stiffness of stiffened panel and therefore the ship global FE model is not sufficient for secondary response analysis and local areas need to be separately analysed with 3D mesh.

Satish Kumar and Mukhopadhyay (2000) added the plate and stiffener bending into the formulation of equivalent plate element by combining the Allman's plane stress element (Allman 1984) with the discrete Kirchhoff-Mindlin triangular plate bending element (Katili 1993) and applied it in the ship static 3D FE analysis. However, the element has several weaknesses. It neglects the coupling between bending and membrane actions. Also, the shear correction factor of 5/6 is used, which does not express the shear stress distribution of stiffened panel correctly. More advanced equivalent elements have been used for web-core sandwich panel response analysis. Lok and Cheng (2000, 2001a, 2001b) derived the expressions for the elastic constants of the symmetric truss-core sandwich panel. The constants represent bending, twisting and transverse shear stiffness and enable the transformation of a 3D structure into an equivalent homogeneous orthotropic thick plate continuum. Romanoff and Varsta (2007) developed a theory for the bending response of asymmetric web-core sandwich structure. The web-core sandwich structure is described as a laminate plate, which follows the thick-face-plate kinematics. The stiffness properties of the sandwich panel were obtained from laminated shell theory (Reddy and Ochoa 1992). Also, the effect of local bending of the face plates was taken into account by adding the local plate response to the overall laminate solution. However, these elements have not been validated for the global strength analysis.

The objective of this paper is to present an equivalent shell element for stiffened panel, where the secondary stiffeners are incorporated into the shell element formulation, to assess ship global and local static and vibration response in limited time frame. Unlike the existing equivalent element formulations for stiffened panels, the element includes the membrane-bending coupling, bending and also shear stiffness, which follows the Reissner-Mindlin plate theory for anisotropic homogenous shells. The relationships between the homogenised internal forces, strains and curvatures are derived according to the laminated shell theory. The local plate bending between the stiffeners is considered by adding the local plate bending response to the laminate element solution. This approach enables FEA of ship structures at primary, secondary and tertiary levels using the same element formulation for all of these levels. This makes the approach suitable in early design stages where various structural analyses are needed. The proposed element is validated with fine mesh analyses based on 3D FEM of the actual geometry without any simplifications. Two case studies are considered. First, a prismatic box-like ship is analysed to test the reliability of the element in global hull girder bending and vibration response analysis. Second, the equivalent element is applied in a typical passenger ship cabin area to prove its suitability for the local response analysis of the ship.

2. Theory

The actual stiffened panel structure is described mathematically using equivalent shell elements, where only homogenised stiffness properties are considered. The in-plane, membrane-bending coupling and bending stiffness of the structure are expressed by *ABD*-matrix and shear stiffness by D_Q-matrix. The stiffness properties are derived with respect to the geometrical mid-plane of the stiffened panel (Figure 2a) and are evaluated only once for each element set containing the same geometrical definition for the stiffened panel.

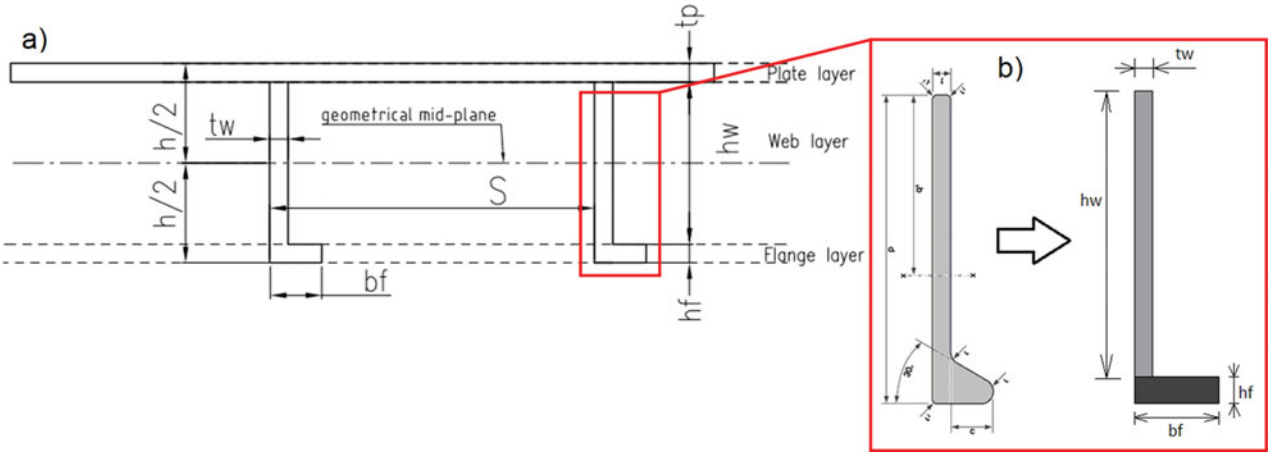

Figure 2. (a) Stiffener panel division into three layer laminate element and the notations used in this paper and (b) the idealisation of the HP-profile flange. (This figure is available in colour online.)

2.1. Notations

The stiffened panel is considered as a three layer laminate element, where the first layer represents the plate, the second layer represents the stiffener web and the third layer represents the stiffener flange. Plate layer has the thickness of the plate t_p, web layer has the thickness of the web height h_w and the flange layer has the thickness of the flange height h_f. The cross section of the flange is idealised as a rectangle, which dimensions result in equal mass and second moment of area as the original HP-profile (Figure 2b).

2.2. Strain-displacement relationship

According to the Kirchhoff plate theory, the displacements *u, v, w* corresponding to the directions *x*, *y* and *z*, respectively, can be expressed as a linear function of the depth *z*:

$$\begin{aligned} u_i &= u_0(x, y) - z_i\theta_x(x, y),\ i = p, w, f, \\ v_i &= v_0(x, y) - z_i\theta_y(x, y),\ i = p, w, f, \\ w &= w(x, y), \end{aligned} \tag{1}$$

where subscript 0 denotes the mid-plane displacements and the slope θ with subscripts x and y describes the rotations around the x and y axis, respectively. The abbreviations p, w and f denote the plate, web and flange, respectively.

The corresponding strain vector $\{\varepsilon\}$ is the gradient of the displacements and it can be written as

$$\begin{Bmatrix} \varepsilon_x \\ \varepsilon_y \\ \gamma_{xy} \end{Bmatrix}_i = \begin{Bmatrix} \varepsilon_x^0 \\ \varepsilon_y^0 \\ \gamma_{xy}^0 \end{Bmatrix}_i + z_i \begin{Bmatrix} \kappa_x \\ \kappa_y \\ \kappa_{xy} \end{Bmatrix},\ i = p, w, f, \tag{2}$$

where $\{\varepsilon\}^0$ is the mid-plane strain vector and $\{\kappa\}$ is the vector of curvature, i.e. the second derivatives of the displacement:

$$\begin{Bmatrix} \varepsilon_x^0 \\ \varepsilon_y^0 \\ \gamma_{xy}^0 \end{Bmatrix} = \begin{Bmatrix} \partial u_0/\partial x \\ \partial v_0/\partial y \\ \partial u_0/\partial y + \partial v_0/\partial x \end{Bmatrix} \qquad \begin{Bmatrix} \kappa_x \\ \kappa_y \\ \kappa_{xy} \end{Bmatrix} = \begin{Bmatrix} -\partial^2 w_g/\partial x^2 \\ -\partial^2 w_g/\partial y^2 \\ -2\partial^2 w_g/\partial x \partial y \end{Bmatrix}. \tag{3}$$

The out-of-plane shear strain can be written as (Whitney and Pagano 1970):

$$\begin{aligned} \gamma_{xz}^i &= -\theta_x + \frac{\partial w_i}{\partial x}, i = p, w, f, \\ \gamma_{yz}^p &= -\theta_y + \frac{\partial w_p}{\partial y}. \end{aligned} \tag{4}$$

2.3. In-plane elasticity matrix

The plate layer is described as a 2D isotropic shell element, where $\varepsilon_z = \gamma_{xz} = \gamma_{yz} = 0$. According to the Hooke's law, the elasticity matrix $[E]$ of the plate layer is

$$[E]_p = \frac{1}{(1-\nu^2)} \begin{bmatrix} E & \nu E & 0 \\ \nu E & E & 0 \\ 0 & 0 & G(1-\nu^2) \end{bmatrix}. \tag{5}$$

The web and flange layers are described as 2D orthotropic shell elements, where the components of the elasticity matrix ($[E]_w$ and $[E]_f$) are found by applying the rule of mixtures:

$$[E]_w = \frac{t_w}{s} \begin{bmatrix} E & 0 & 0 \\ 0 & 0 & 0 \\ 0 & 0 & 0 \end{bmatrix}, \tag{6}$$

$$[E]_f = \frac{b_f}{s} \begin{bmatrix} E & 0 & 0 \\ 0 & 0 & 0 \\ 0 & 0 & 0 \end{bmatrix}. \tag{7}$$

The normal stress vector $\{\sigma\} = \{\sigma_x\ \sigma_y\ \tau_{xy}\}^T$ for layer i is obtained by multiplying the strains $\{\varepsilon\} = \{\varepsilon_x\ \varepsilon_y\ \gamma_{xy}\}^T$ with the elasticity matrices $[E]$:

$$\{\sigma\}_i = [E]_i \{\varepsilon\}_i,\ i = p, w, f. \tag{8}$$

2.4. Relationship between the internal forces and strains

Internal forces and moments in the laminated plate are related to the stresses in the layer and to the deformations in the laminate and they are obtained by integrating Equation (8) over the thickness of the stiffened panel. The normal force vector $\{N\} = \{N_x\ N_y\ N_{xy}\}^T$ is then:

$$\{N\} = \int_{-h/2}^{h/2} [E]_i \{\varepsilon\}_i \, dz, i = p, f, w \tag{9}$$

and the bending moment vector $\{M\} = \{M_x\ M_y\ M_{xy}\}^T$ is

$$\{M\} = \int_{-h/2}^{h/2} [E]_i\, z \{\varepsilon\}_i \, dz,\ i = p, f, w. \tag{10}$$

Taking into account Equation (2), the normal force becomes

$$\{N\} = [A]\{\varepsilon_0\} + [B]\{\kappa\}. \tag{11}$$

Similar expression can be written for the moment resultants:

$$\{M\} = [B]\{\varepsilon_0\} + [D]\{\kappa\}, \tag{12}$$

where the stiffness matrices are

$$[A] = \int_{-h/2}^{h/2} [E]_i \, \mathrm{d}z, \, i = \mathrm{p, w, f}. \tag{13}$$

$$[B] = \int_{-h/2}^{h/2} [E]_i \, z_i \mathrm{d}z, \quad i = \mathrm{p, w, f}, \tag{14}$$

$$[D] = \frac{1}{3} \int_{-h/2}^{h/2} [E]_i \, z_i^2 \mathrm{d}z, \quad i = \mathrm{p, w, f}. \tag{15}$$

Inserting elasticity matrices, Equations (5), (6) and (7), into the *ABD*-matrix expressions, Equations (13), (14) and (15), the $[A]$, $[B]$ and $[D]$ stiffness matrices for stiffened panel are obtained:

$$[A] = \int_{-h/2}^{-h/2+h_f} [E]_f \mathrm{d}z + \int_{-h/2+h_f}^{h/2-t_p} [E]_w \mathrm{d}z + \int_{h/2-t_p}^{h/2} [E]_p \mathrm{d}z, \tag{16}$$

$$[B] = \int_{-h/2}^{-h/2+h_f} [E]_f z \mathrm{d}z + \int_{-h/2+h_f}^{h/2-t_p} [E]_w z \mathrm{d}z + \int_{h/2-t_p}^{h/2} [E]_p z \mathrm{d}z, \tag{17}$$

$$[D] = \int_{-h/2}^{-h/2+h_f} [E]_f \, z^2 \mathrm{d}z + \int_{-h/2+h_f}^{h/2-t_p} [E]_w z^2 \mathrm{d}z + \int_{h/2-t_p}^{h/2} [E]_p \, z^2 \mathrm{d}z. \tag{18}$$

Because the plate and stiffener layers have the same material orientation angle, which is 0 or 90°, the terms 16, 61, 26 and 62 of *ABD* matrices are zero in Equations (16)–(18). Thus, the applied axial forces cause no shear strains and the applied shear forces cause no axial strains.

2.5. *Relationship between out-of-plane shear forces and shear strains*

An additional deflection will be produced by the shearing force, Q_z, due to the mutual sliding of adjacent cross sections along each other. This phenomenon can be taken into account by applying Reissner-Mindlin plate theory. According to that the relationship between the shear force $\{Q_Q\}$ and average shear strain $\{\gamma\}$ is written as (Whitney and Pagano 1970):

$$\begin{Bmatrix} Q_{Q,x} \\ Q_{Q,y} \end{Bmatrix} = \begin{bmatrix} D_{Qx} & 0 \\ 0 & D_{Qy} \end{bmatrix} \begin{Bmatrix} \gamma_{xz} \\ \gamma_{yz} \end{Bmatrix}, \tag{19}$$

where D_{Qx} is the shear stiffness of laminate in stiffener direction and D_{Qy} transverse to stiffener direction.

2.5.1. *Shear stiffness in the stiffener direction*

The shear stiffness D_{Qx} can be written as

$$D_{Qx} = k_{xz} \left(G_p t_p + G_w h_w + G_f h_f \right), \tag{20}$$

where G_p is the shear modulus for the plate layer and G_w and G_f are the shear modules for web and flange layers, respectively. These can be obtained from the following relations:

$$G_w = G_s \frac{t_w}{s}, \qquad G_f = G_s \frac{b_f}{s}. \tag{21}$$

k_{xz} is the shear correction factor in the xz-plane. Shear correction factor k relates the maximum shearing stress $(\tau_{xz})_{\max}$, i.e. the shearing stress at the centroid of the cross section, to the average stress $(\tau_{xz})_{\mathrm{avg}}$:

$$k = \frac{(\tau_{xz})_{\mathrm{avg}}}{(\tau_{xz})_{\max}}. \tag{22}$$

For stiffened panel structure, the average shear stress can be calculated from

$$(\tau_{xz})_{\mathrm{avg}} = \frac{\int_0^h \tau_{xz}(z) \mathrm{d}z}{h}, \tag{23}$$

where h is the total length of the shear flow area in xz-plane, which for stiffened panel structure is equal with $h = t_p + h_w + h_f$. The average shear stress can also be obtained by using the well-known approach by dividing the shear force by the effective shear area:

$$(\tau_{xz})_{\mathrm{avg}} \approx \frac{Q_z}{A_w + t_w t_p + t_w h_f}. \tag{24}$$

The maximum shear stress $(\tau_{xz})_{\max}$ in stiffened panel is defined as

$$(\tau_{xz})_{\max} = \frac{Q_z \left[A_p (2 z_{na} - t_p) + t_w (z_{na} - t_p)^2 \right]}{2 I_z t_w}, \tag{25}$$

where z_{na} is the distance from the neutral axis and I_z is the second moment of area. Shear correction factor in stiffener direction depends on different parameters such as plate thickness, effective breadth of the plate and stiffener type. It is found here that it varies between 0.7 and 0.8, being smaller when the stiffener spacing and the plate thickness is smaller and being larger in the structures, where the neutral axis is more close to the plate surface.

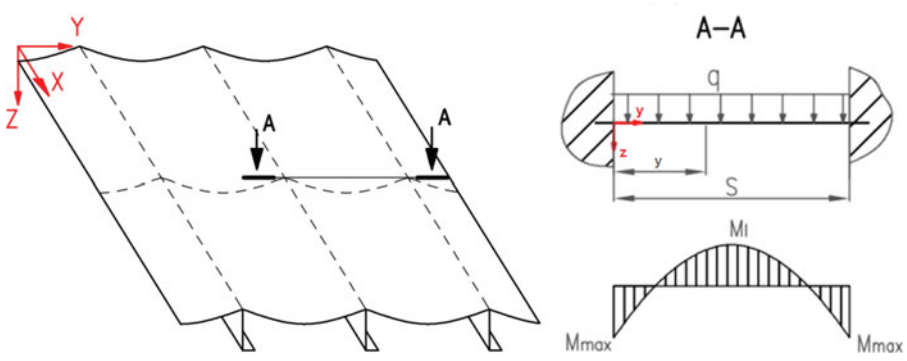

Figure 3. Local bending of the deck plate. (This figure is available in colour online.)

2.5.2. *Shear stiffness transverse to stiffener direction*

Due to discontinuity of the web and flange layers transverse to the stiffener direction their participation in the laminate shear stiffness D_{Qy} can be neglected and it becomes

$$D_{Qy} = k_{yz}(G_p t_p), \tag{26}$$

where the shear correction factor k_{yz} 5/6 is derived from the plate shear energy and is included in Reissner-Mindlin plate theory (Whitney and Pagano 1970).

2.6. *Relationship between homogenised internal forces and strains and curvatures*

If $[A]$, $[B]$, $[D]$ and shear stiffness matrix $[D]_Q$ are obtained, the Equations (11), (12) and (19) can be summarised as a single matrix form

$$\begin{Bmatrix} N \\ M \\ Q \end{Bmatrix} = \begin{bmatrix} A & B & 0 \\ B & D & 0 \\ 0 & 0 & D_Q \end{bmatrix} \begin{Bmatrix} \varepsilon \\ \kappa \\ \gamma \end{Bmatrix}. \tag{27}$$

2.7. *Local bending of the deck plate*

Due to lateral loads an additional plate bending between the stiffeners occurs (Figure 3), which cannot be predicted by the homogenised model, where it is assumed that the stiffener spacing divided by the panel breadth equals zero ($s/B = 0$) (see Romanoff et al. 2007). In global ship analysis such tertiary effects are usually neglected, because the main focus is on the primary and secondary response. However, if the plate top or bottom stress is of interest, then the previously described theory is limited and the additional bending response should be included.

The total stress of the plate layer is found by adding the local plate bending stresses to the laminate solution, i.e.

$$\begin{Bmatrix} \sigma_x^{\text{tot}} \\ \sigma_y^{\text{tot}} \\ \tau_{xy}^{\text{tot}} \end{Bmatrix}_i = \begin{Bmatrix} \sigma_x^{g} \\ \sigma_y^{g} \\ \tau_{xy}^{g} \end{Bmatrix}_i + \begin{Bmatrix} \sigma_x^{l} \\ \sigma_y^{l} \\ \tau_{xy}^{l} \end{Bmatrix}_i, i = t, b, \tag{28}$$

where subscripts t and b denote top and bottom surface, respectively. Superscript g and l denote the global and local deflection, respectively. The local term to be superimposed to the global can be calculated using analytical expressions available, e.g. in basic books of plate theory or using small FE sub-model.

The total deflection in the plate thickness direction, w_{tot}, is obtained by the same principle:

$$w_{\text{tot}} = w_g + w_l. \tag{29}$$

3. Case studies

3.1. *General*

Two case studies are considered. In the first, box-beam-ship in four-point-bending is used to validate the global response of the hull girder using laminate element mesh and 3D fine mesh. In the second case, the response of passenger ship cabin area is considered using the same methods. Stiffness, stress and vibration responses are considered. The mass matrix is formulated using the lumped scheme, where the distributed mass of the element is simply divided between the nodes. According to that, a diagonal mass matrix is built, which provides higher computational economy. The FE analysis is carried out using NX Nastran 7.1 software. The pre- and post-processing is done with FEMAP 10.2.

3.1.1. *Laminate element models*

The stiffened panel is modelled using laminate shell element (CQUAD4), which has four nodes and 24 DOF.

Table 1. Laminate element material properties of the box-like ship.

Layer	E [Pa]		G [Pa]			
	x	Y	xy	xz	yz	ρ [kg/m^3]
Plate	2.06×10^{11}	2.06×10^{11}	7.92×10^{10}	7.92×10^{10}	7.92×10^{10}	8000
Web	2.47×10^{9}	–	–	8.86×10^{8}	–	96.0
Flange	9.62×10^{9}	–	–	3.45×10^{9}	–	374

Table 2. Laminate element material properties of the deck structure.

Layer	E [Pa]		G [Pa]			
	x	Y	xy	xz	Yz	ρ [kg/m^3]
Plate	2.06×10^{11}	2.06×10^{11}	7.92×10^{10}	7.92×10^{10}	7.92×10^{10}	7850
Web	1.59×10^{9}	–	–	5.74×10^{8}	–	60.6
Flange	6.10×10^{9}	–	–	2.20×10^{9}	–	232.3

Calculated material properties are presented in Table 1 and Table 2 for the box-beam-ship and the cabin area, respectively. Primary stiffeners of the structure are modelled using offset beam elements (CBEAM), which follow Timoshenko theory (see Figure 4). In order to investigate mesh sensitivity on box-beam-ship, two laminate models are created. In the first model, the mesh density is eight ($le = 0.313$ m) and in the second two elements ($le = 1.25$ m) per web spacing (see Figure 5). The models consist of 16,440 DOF and 1194 DOF, respectively. For the cabin area investigations, the mesh size is 85 mm, which means 175,302 DOF.

3.1.2. *3D fine mesh model*

The 3D fine mesh model is created using four-node shell elements (QUAD4) for plating and stiffener and girder webs and offset beam elements (CBEAM) for stiffener and girder flanges (see Figure 5a). For box-beam-ship, the mesh size is 100 mm, which is 25 elements per web spacing. The girder webs have three elements and stiffener webs one element in height (z) direction. The total DOF of the model is 195,072. In cabin area calculations, the mesh size is 85 mm, which is eight elements per stiffener spacing. The girder webs have five elements and stiffener webs one element in height (z) direction. The model consists of 226,452 DOF.

3.2. *Box-like ship*

3.2.1. *Case definition*

The structure of the box ship is shown in Figure 6. It has rectangular cross-section with the plate thickness of 6 mm. The structure is stiffened with HP-profiles HP100 × 6 and girders T300 × 8/150 × 10. Stiffener spacing is 500 mm and frame spacing is 2500 mm. The ship is made of steel with Young's modulus of 206 GPa, Poisson ratio of 0.3 and mass density of 8000 kg/m^3.

In order to analyse the hull bending response, four-point bending test is carried out. The hull girder is considered as

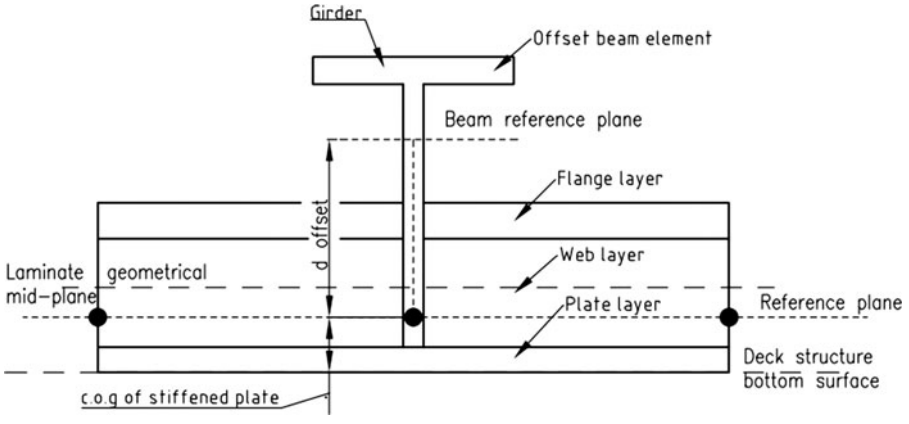

Figure 4. Stiffened panel modelled as laminate element and T-girder as offset beam.

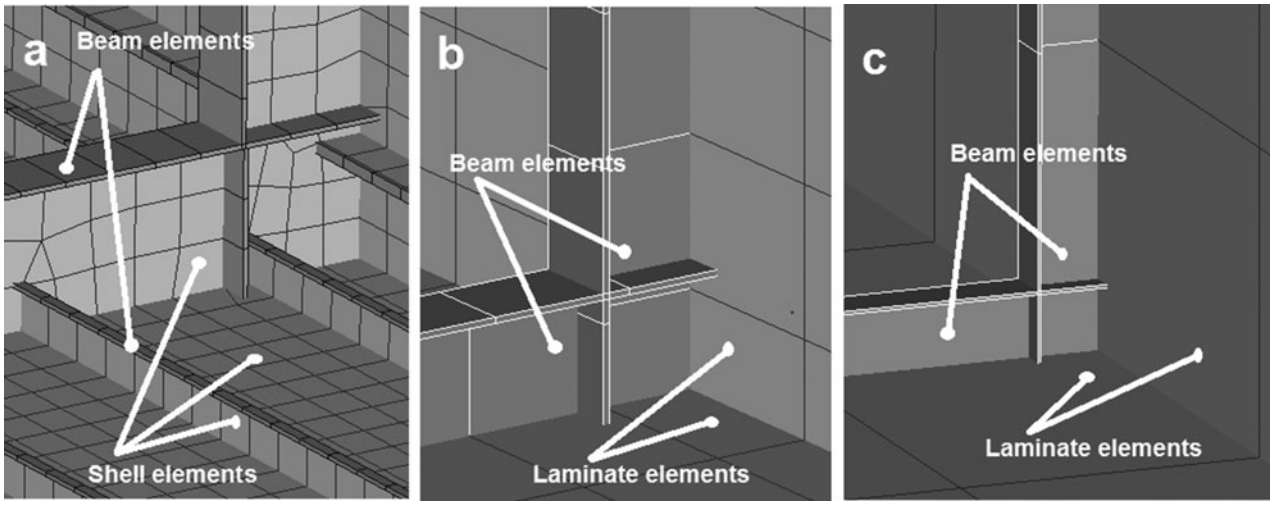

Figure 5. Mesh density in (a) fine mesh, (b) laminate model (eight elements per frame) and (c) laminate model (two elements per frame).

a beam and two similar unit loads of 1 MN are applied at regions $x = 5$ m and $x = 12.5$ m (Figure 7). These loads produce a uniform bending moment of 5 MNm over the mid section. The maximum shear force is 1 MN.

3.2.2. *Static response*

The analysis results indicate that the maximum deflection as well as the deflection distribution agrees very well between laminate and fine mesh model (Figure 8). The maximum deflection in coarser laminate model is 15.1 mm, which is 1.6% more than the corresponding value from the fine mesh model. Nevertheless, the coarser laminate model consists of 176 times less DOF, which provides remarkable computational time saving.

Figure 9 presents the side shell x-normal stresses at the mid ship ($x = L/2$). Both the shape and the magnitude of the stresses are in good agreement with the fine mesh results

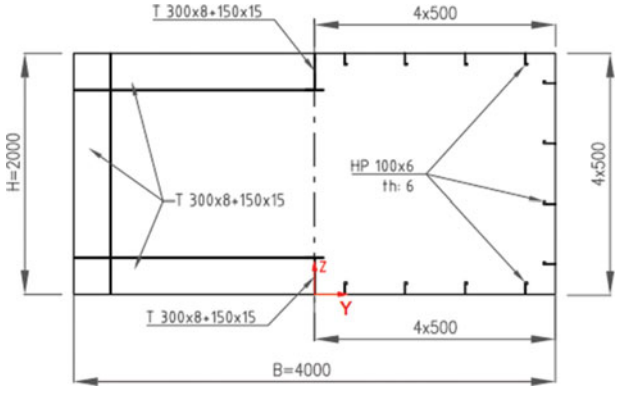

Figure 6. Midframe of box-like ship, the ship total length is L = 17.5 m and the web frame spacing is 2.5 m. (This figure is available in colour online.)

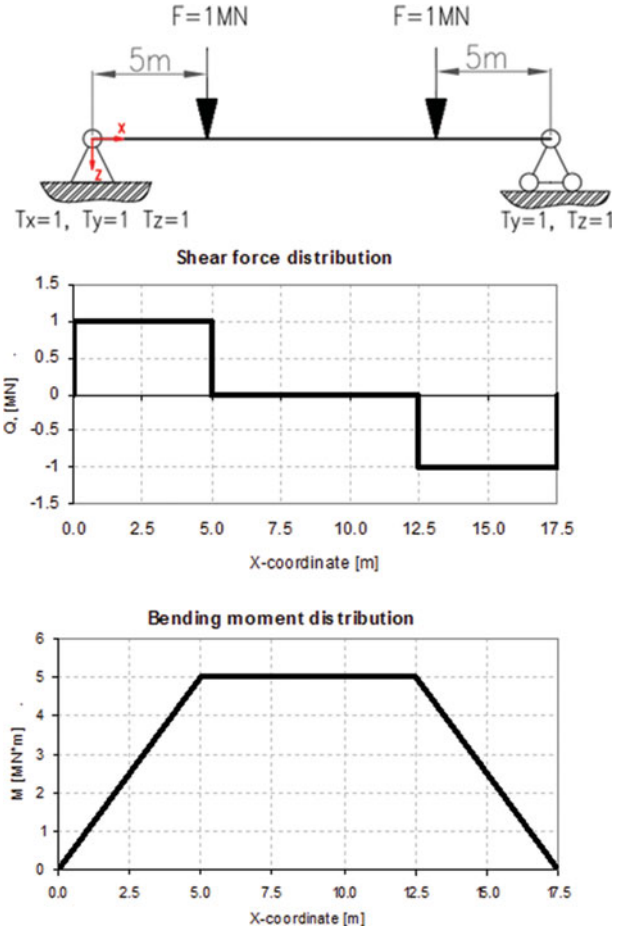

Figure 7. Four-point bending load for the box-like ship. (This figure is available in colour online.)

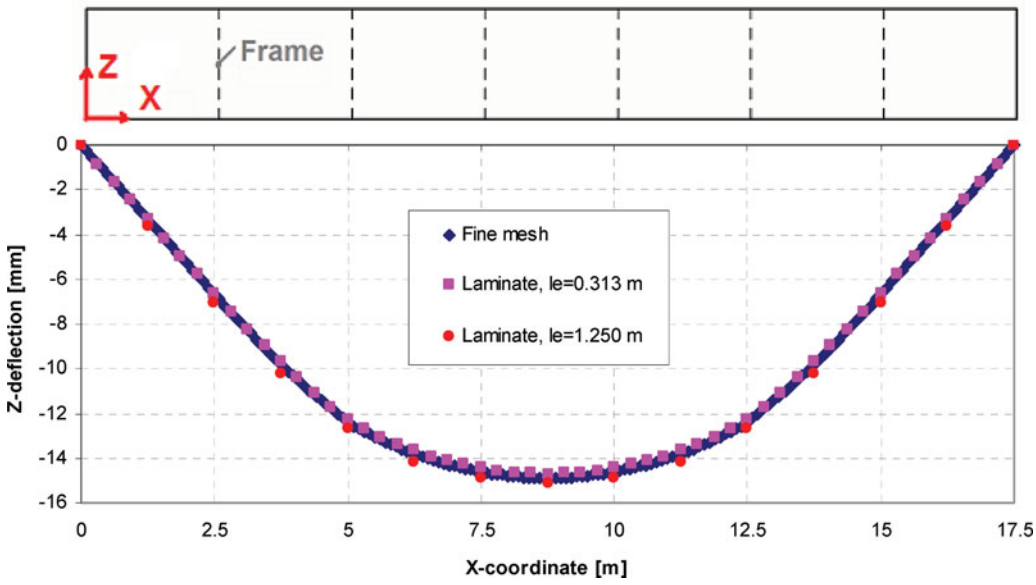

Figure 8. The deflection of the box-like ship. (This figure is available in colour online.)

and the maximum stress is evaluated with less than 0.7% ($le = 0.313$ m) and 0.5% ($le = 1.25$ m) difference. Finally, the shear stresses, τ_{xy}, in ship side shell are analysed. The shear stress distribution and values show good agreement between laminate and fine mesh models as well (see Figure 10). The results also reveal that with proper mesh size the laminate element is able to predict the shear stresses due to secondary effects, i.e. the local bending of the stiffened panel between the web frames. The maximum shear stress in finer mesh laminate model ($le = 0.313$ m) is evaluated with 1.3% difference from fine mesh results. However, in the case of coarser mesh, the difference increases to 11.3%.

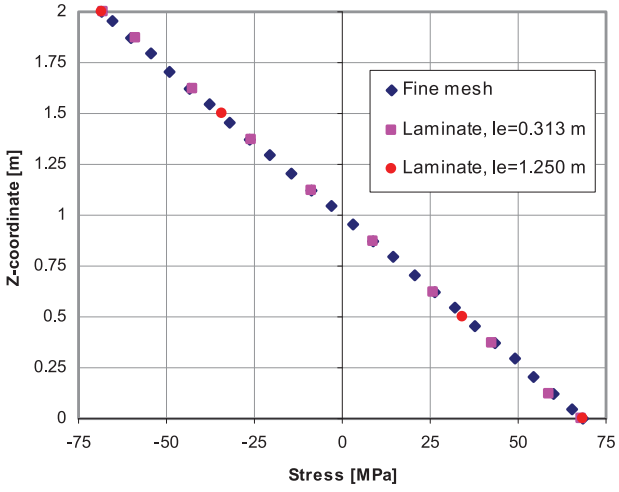

Figure 9. Comparison of x-directional stress distribution, σ_x, in $x = L/2$. (This figure is available in colour online.)

3.2.3. *Hull girder natural frequency analysis*

Five most important dry frequencies are analysed using the fine mesh model and the laminate models with two different mesh densities (see Figure 5). The results are listed in Table 3 and the vibration mode shapes are presented graphically in Figure 11. The natural frequencies calculated using the laminate element models agree well with the fine mesh ones. The largest difference, 9.3%, occurs in the third mode, which describes the shear vibration of ship sections. Since primary stiffeners have strong influence on mid section shear stiffness, the major part of that error is due to too coarse mesh. The differences in rest of the modes vary from -0.6% to -5.6%.

3.3. *Passenger ship cabin area*

3.3.1. *Case description*

The thickness of the deck plate is 6 mm and it is stiffened with HP100×6 profiles with the spacing of 680 mm. The web frame (T-440 × 7 + FB150 × 10) spacing is 2400 mm and a pillar (Ø150 × 15) is located at every second frame. All structural parts are made of steel with Young's modulus of 206 GPa, Poisson ratio of 0.3 and mass density of 7850 kg/m^3. All edges of the model have clamped boundary conditions. The local coordinate system and its origin is shown in Figure 12a.

3.3.2. *Bending response*

The deck plating is loaded with uniform pressure of $q =$ 10 kPa. The analysis results indicate that the maximum deflection as well as the deflection distributions can be

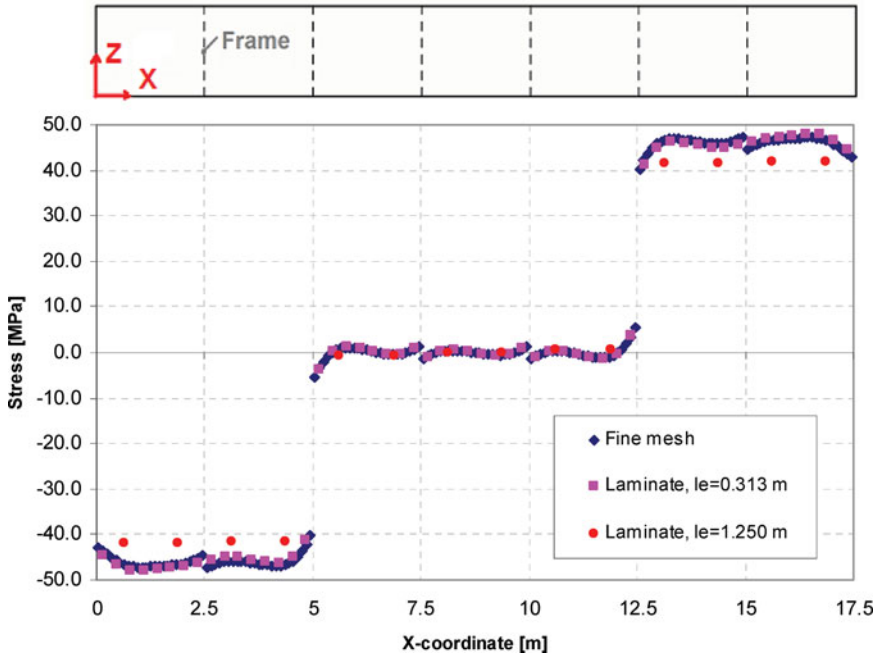

Figure 10. Comparison of shear stress distribution, τ_{xy}, in $z = H/2$ in x-direction. (This figure is available in colour online.)

predicted with good accuracy using the laminate mesh (Figure 13). The maximum deflection in x-direction, measured at the longitudinal girder ($y = 0$ m), is evaluated with less than 3% and at the stiffener line ($y = 2.72$ m) with less than 1% difference compared to the fine mesh model (Figure 13a). The deflections in y-direction show good agreement as well and the maximum deflection at the transversal girder ($x = 7.2$ m) is evaluated with less than 3% difference. The local plate bending between the stiffeners is also successfully taken into account and the maximum deflection at $x = 8.4$ m are predicted with less than 1% difference (Figure 13b).

Figure 14 presents the normal stresses in x-direction at the mid, top and bottom surfaces of the deck plate at $y = 2.72$ m. Both the shape and the magnitude of the stresses are in good agreement with the fine mesh results. The results reveal that the maximum membrane stress of the deck plate is significantly lower than the local bending stress. Therefore, it is very important to consider the local plate bending, especially when the plate thickness is small and stiffener spacing is large. Figure 15 shows the average normal stresses in stiffener flange at $y = 2.72$ m. Again, both the shape and the maximum stress are predicted with good accuracy. The average difference from 3D FE model is about 8%. Figure 16 compares the shear stresses, τ_{xy}, in deck plate and the maximum bottom stress is evaluated with less than 2% difference.

3.3.3. *Natural frequency analysis*

Four most important frequencies are analysed using the fine mesh model and the laminate models with three different mesh densities: eight elements ($le = 0.085$ m) and one element ($le = 0.680$ m) per stiffener spacing and two elements

Table 3. Natural frequencies (Hz) for the box-like ship.

	Fine mesh	Laminate: $h = 0.313$ m		Laminate: $h = 1.25$ m	
Mode no.	[Hz]	[Hz]	Dif. [%]	[Hz]	Dif. [%]
1	30.26	30.08	−0.6	29.98	−0.9
2	33.44	31.81	−4.9	32.63	−2.4
3	40.06	36.43	−9.1	36.33	−9.3
4	44.17	43.63	−1.2	42.32	−4.2
5	44.52	43.61	−2.0	42.01	−5.6

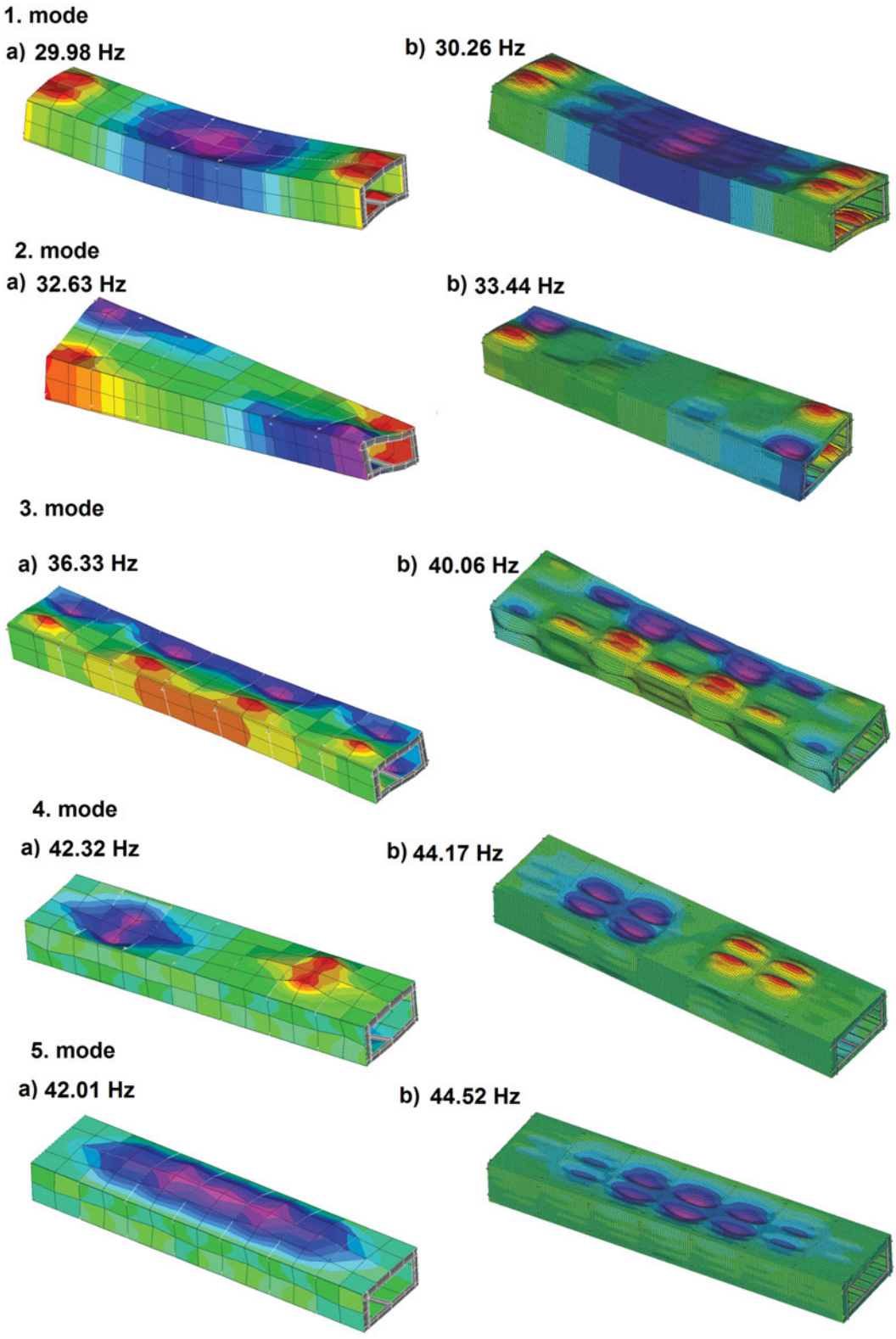

Figure 11. Analysed vibration modes with (a) laminate element model ($le = 1.25$ m) and (b) fine mesh model. (This figure is available in colour online.)

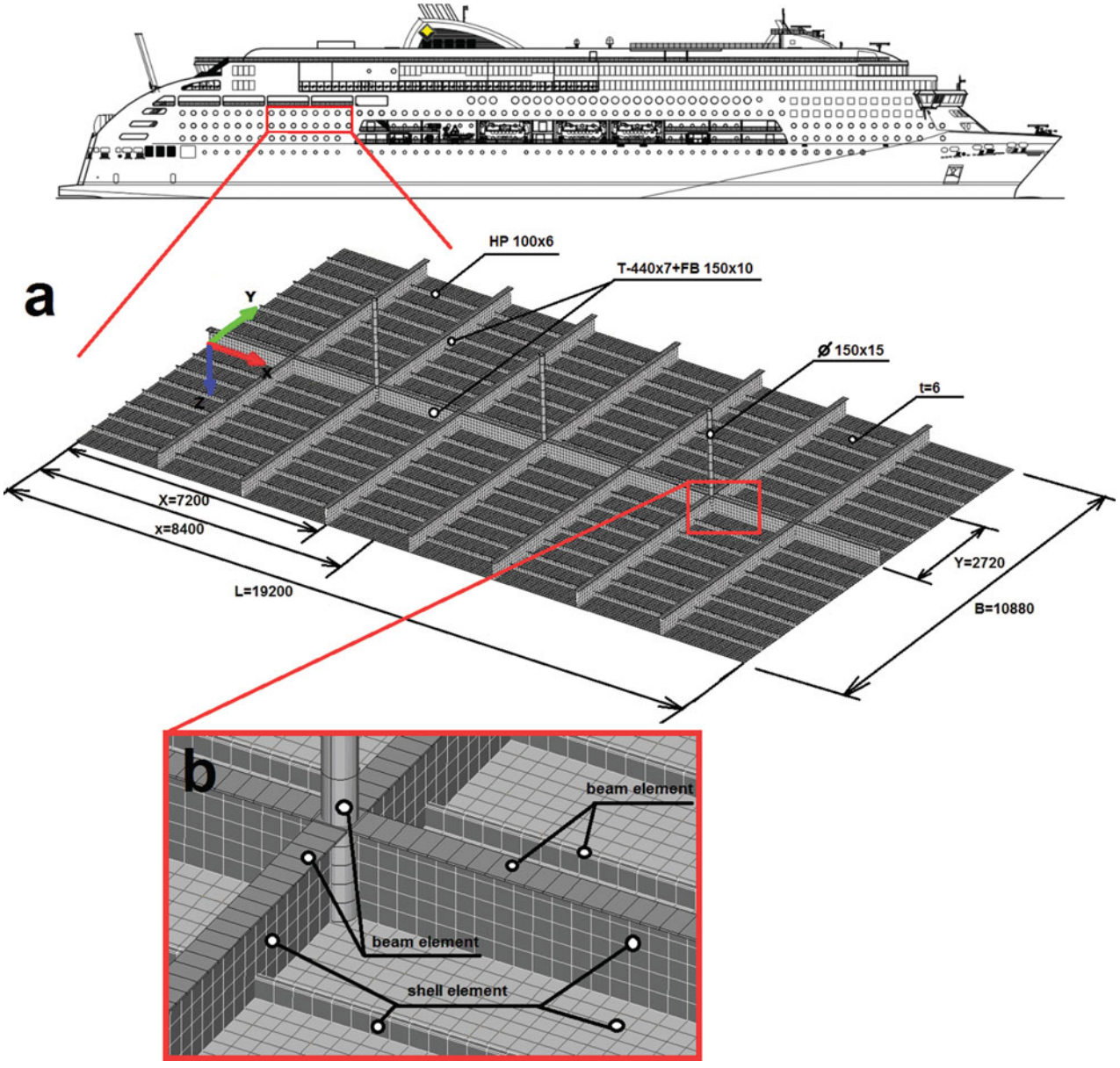

Figure 12. (a) The dimensions of the deck structure (mm) and local coordinate system; (b) mesh density in fine mesh model. (This figure is available in colour online.)

($le = 1.20$) per web frame spacing. The results are listed in Table 4 and the mode shapes are presented graphically in Figure 17. Generally, the natural frequencies calculated using the laminate element models agree well with the fine mesh ones, even if only four laminate elements are used to describe the vibration shape (two elements per web frame). The global modes are captured with less than 2% accuracy. In higher modes, where the local plate vibration between stiffeners becomes more active, the laminate model results start slightly deviating from the 3D-FE solution and the natural frequencies are evaluated with 3.6% to 8.6% difference. It can be seen that in the case of coarser mesh, the laminate model gives better results. This could be explained by the use of lumped mass distribution, where the element mass is equally divided between nodes. If the mesh is coarse then the mass is more concentrated into the centre. This lowers the natural frequencies. At the same time larger elements make the structure stiffer. These two errors with opposite signs compensate each other to some extent.

4. Discussion

The equivalent shell element presented in this paper is able to assess ship global and local static and vibration response

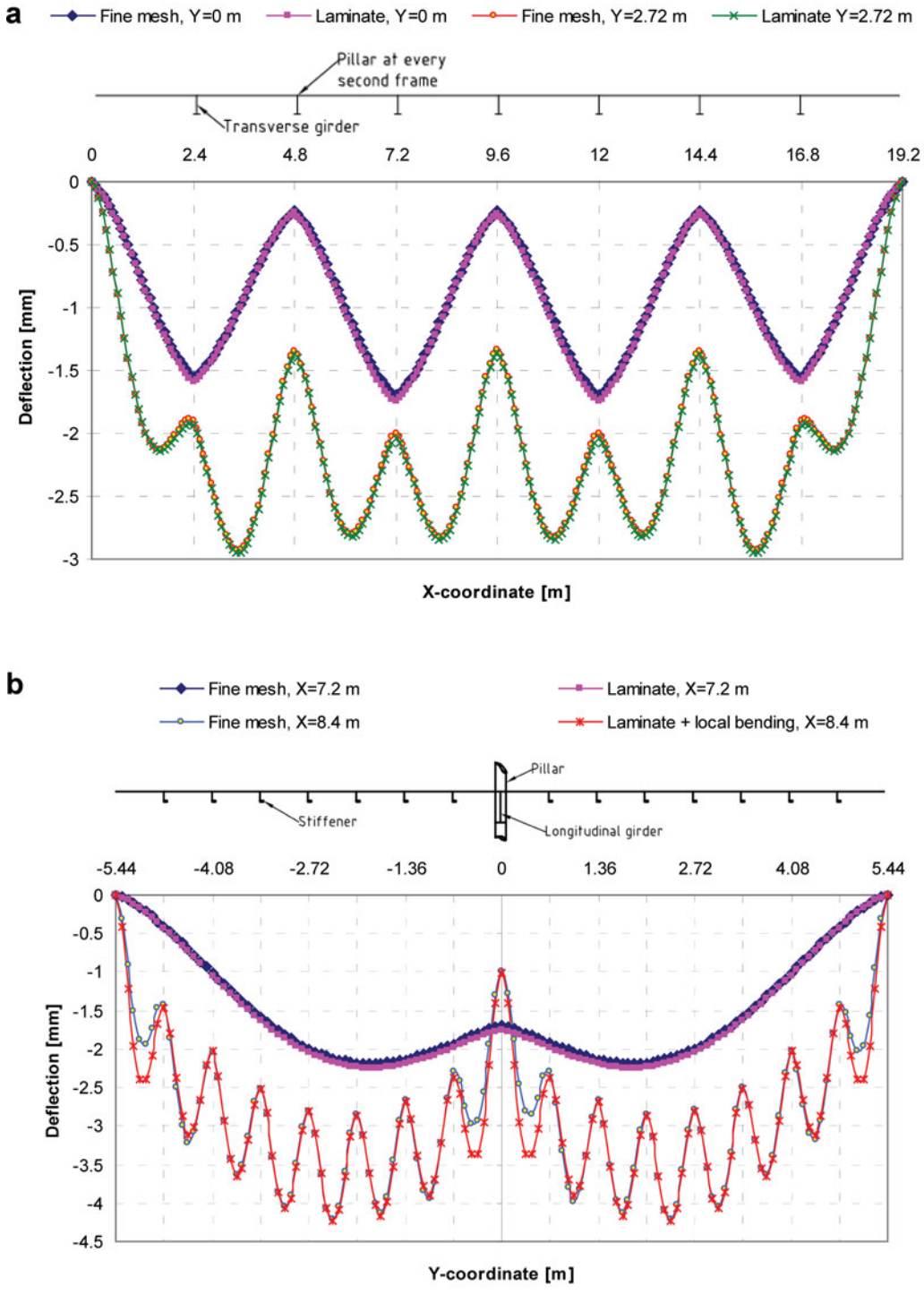

Figure 13. The deflection of the deck structure under uniform pressure loading of $q = 10$ kPa in (a) x-direction and (b) y-direction. (This figure is available in colour online.)

accurately and relatively fast, i.e. in the present investigation with up to 190 times less DOF. Also the possible changes, such as modifying the stiffener type or spacing, can be performed quickly without re-meshing the model. This offers significant time saving and makes present equivalent element very suitable in early design phases. The mesh sensitivity analysis showed that two 4-noded elements per web frame are an optimal size to evaluate the lower natural

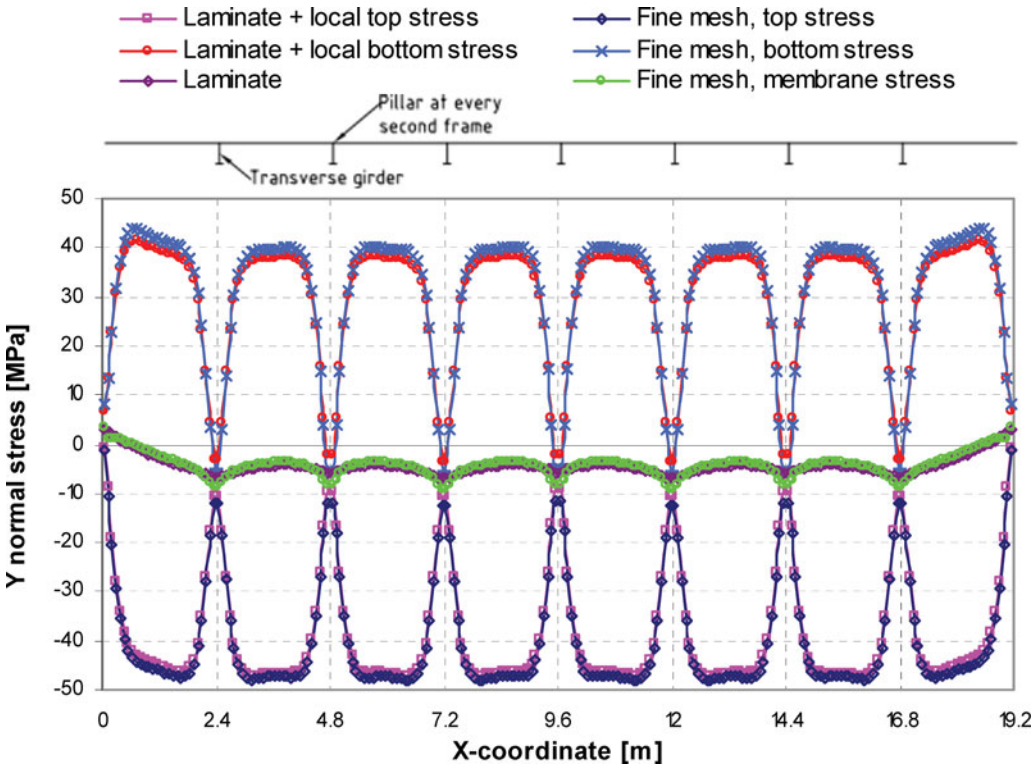

Figure 14. Comparison of deck plating normal stress distribution, σ_y, at $y = 2.72$ m. (This figure is available in colour online.)

frequencies of deck structure with good accuracy. Therefore, this mesh density is recommended for global FE model if secondary responses are of interest. This mesh size recommendation is denser than that recommended by classification society rules (DNV 2007) and for example by Payer (1968) and McVee (1980). However, this more dense mesh size is justified when the response of primary, secondary and tertiary levels are to be analysed using the same FE mesh.

Compared to existing equivalent elements (e.g. Hughes 1988) the developed element includes membrane-bending coupling, which stiffness properties have been calculated using laminated shell theory. Due to layerwise-formulation, it is possible to extract the normal and shear stresses from plate, stiffener web and flange separately. Second, local plate bending between the stiffeners is added to the overall laminate solution. This enables to analyse the tertiary response, i.e. deck plate top and bottom stresses straight from the global model and loses the need for the tedious sub-modelling (Mobasher et al. 2009). The shear correction factor in stiffener direction is calculated and gets values between 0.7 and 0.8 which are different from that of 5/6 proposed by Satish Kumar and Mukhopadhyay (2000).

The present paper compared the static response and natural frequencies obtained using laminate element and shell models of the actual 3D geometry. More detailed comparison could be carried out considering for example the lumped stiffener method often used in practical design. However, this investigation is left for future work. In the case of vibration, the laminate element results start to deviate from the fine mesh solution in higher modes where the plate between the stiffeners starts to actively vibrate. These local effects can probably be taken into account in the same manner as in static analysis. From the orthotropic material

Table 4. Natural frequencies (Hz) for the deck structure.

	Fine mesh	Laminate $h = 0.085$		Laminate $h = 0.680$		Laminate $h = 1.200$	
Mode no.	[Hz]	[Hz]	Dif. [%]	[Hz]	Dif. [%]	[Hz]	Dif. [%]
1	32.5	33.0	1.5	32.5	−0.2	31.9	−2.0
2	34.2	34.5	1.1	33.9	−0.7	33.5	−2.0
3	38.4	41.4	7.6	40.3	4.8	39.8	3.6
4	39.0	42.4	8.6	41.2	5.6	40.6	4.1

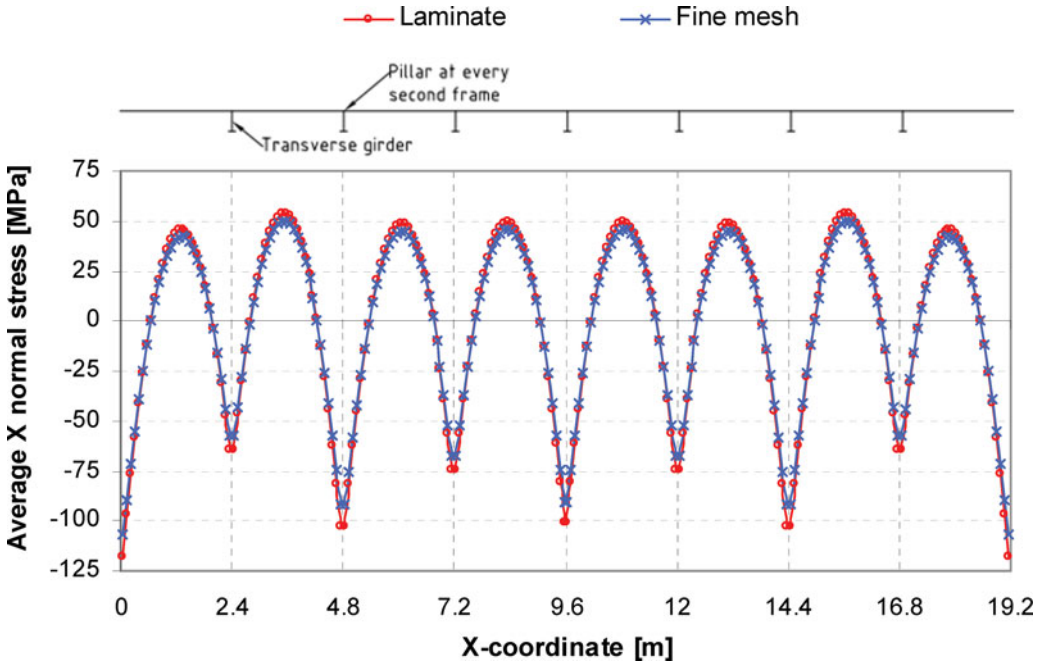

Figure 15. Average normal stresses, σ_x, in stiffener flange at $y = 2.72$ m. (This figure is available in colour online.)

properties it is possible to derive stiffener parameters such as spacing and the thickness of web and flange. Therefore, the utilisation of the laminate element in the optimisation process of the ship structures seems possible and attractive. Future work may also be done for including fluid effects in the vibration analysis.

Acknowledgements

The research work carried out in this paper was funded by STX Turku Shipyard in the FIMECC project Sustainable Breakthrough Innovations. The financial support is gratefully appreciated.

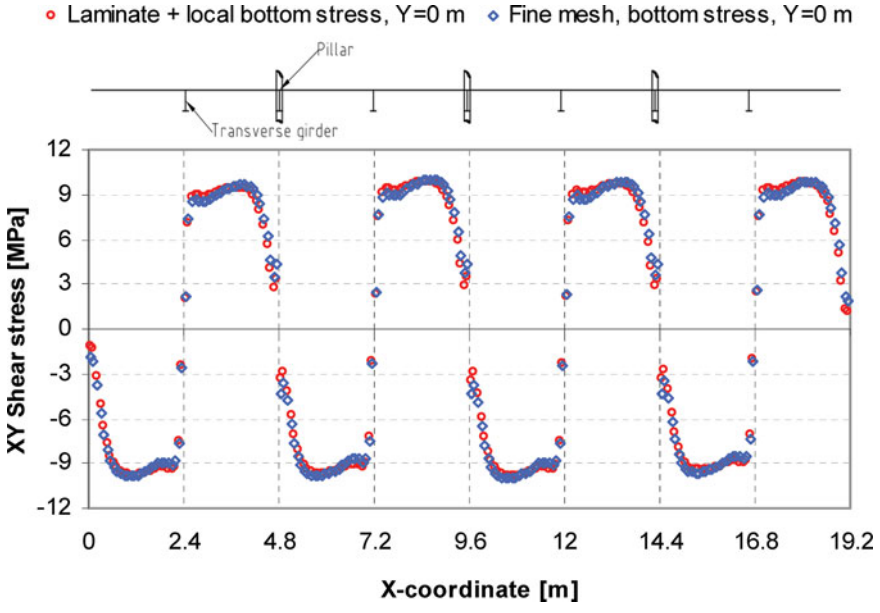

Figure 16. Comparison of deck plating shear stress distribution, τ_{xy}, at $y = 0$. (This figure is available in colour online.)

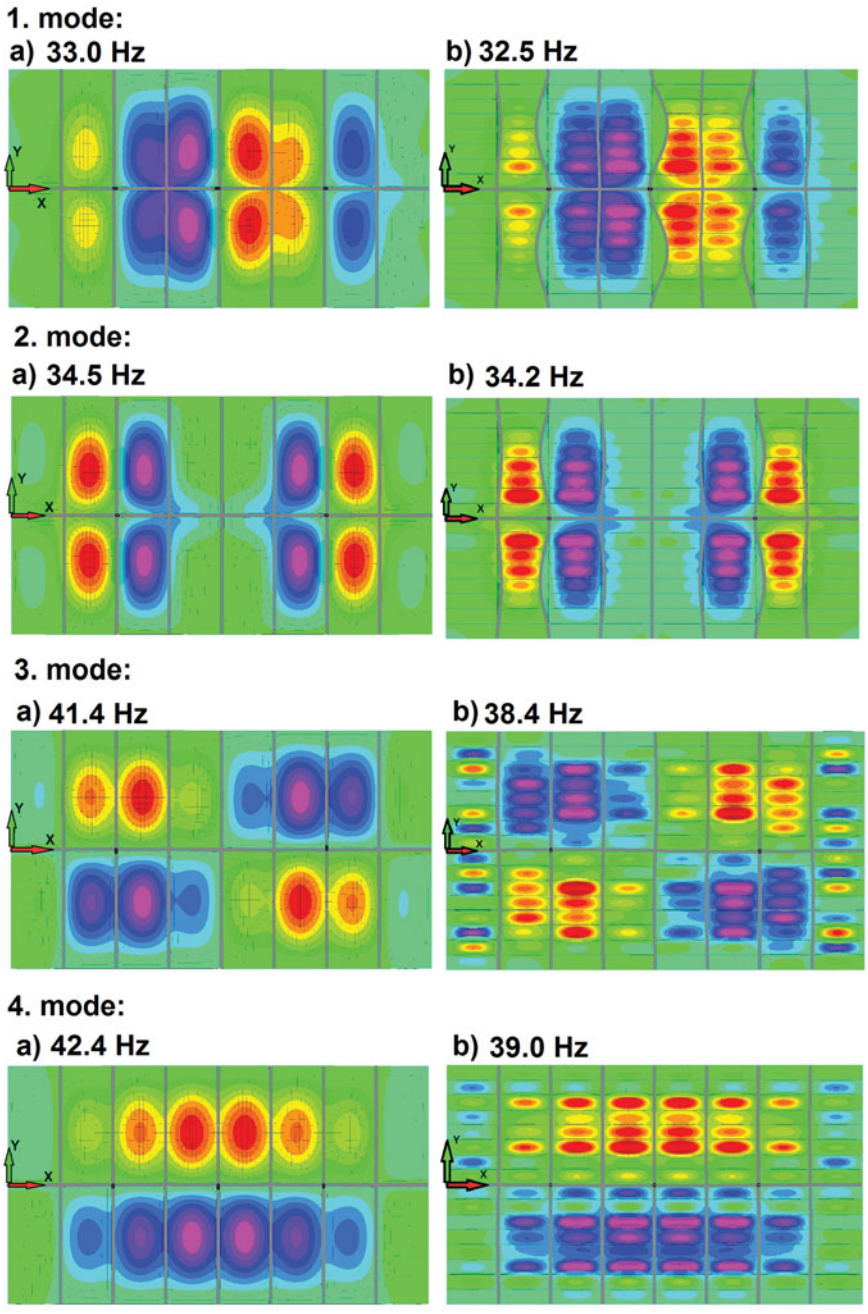

Figure 17. Analysed vibration modes with (a) laminate element model ($le = 0.085$ m) and (b) fine mesh model. (This figure is available in colour online.)

References

Allman DJ. 1984. A compatible triangular element including vertex rotations for plane elasticity analysis. Comput Struct. 19(1/2):1–8.

Andric J, Zanic V. 2010. The global structural response model for multi-deck ships in concept design stage. Ocean Eng. 37:688–704.

Det Norske Veritas. 2007. Direct strength analysis of hull structures in passenger ships. Classification Notes no.31.8. Høvik, Norway.

Det Norske Veritas. 2013. Rules for classification of ships. Part 3, Ch. 1. Høvik, Norway.

Fransman J. 1988. The influence of passenger ship superstructures on the response of the hull girder. Trans RINA. 131:1–12.

Gudmunsen MJ. 2000. The structural design of large passenger ships. London: Lloyds Register of Shipping.

Heder M, Ulfvarson A. 1991. Hull beam behavior of passenger ships. Mar Struct. 4:17–34.

Hughes OF. 1988. Ship structural design: a rationally-based, computer-aided, optimization approach. New Jersey, NJ: The

Society of Naval Architects and Marine Engineers.
Hughes OF, Mistree F, Zanic V. 1980. A practical method for the rational design of ship structures. J Ship Res. 24(2):101–113.
ISSC. 1997. Committee II. 1 – quasi-static response. Proceedings of the 13th International Ship and Offshore Structures Congress, Pergamon Press (Elsevier), Oxford, UK.
Jang BS, Suh YS, Kim EK, Lee TH. 2008. Automatic FE modeler using stiffener-based mesh generation algorithm for ship structural analysis. Mar Struct. 21:294–325.
Katili I. 1993. A new discrete Kirchhoff-Mindlin element based on Mindlin-Reissner plate theory and assumed shear strain fields-part I: an extended DKT element for thick-plate bending analysis. Int. J. Numer. Methods Eng. 36(11):1859–1883.
Kurki T. 2010. Utilization of integrated design and mesh generation in ship design process. J Struct Mech. 43(3):129–139.
Lok TS, Cheng QH. 2000. Free vibration of clamped orthotropic sandwich panel. J Sound Vib. 229(2):311–327.
Lok TS, Cheng QH. 2001a. Bending and forced vibration response of clamped orthotropic thick plate and sandwich panel. J Sound Vib. 245(1):63–78.
Lok TS, Cheng QH. 2001b. Free and forced vibration of simply supported, of orthotropic sandwich panel. Comput Struct. 79:301–312.
McVee JD. 1980. A finite element study of hull-deckhouse interaction. Comput Struct. 12:371–393.
Mobasher AA, Dureisseix D, Cartraud P, Buannic N. 2009. A domain decomposition method for problems with structural heterogeneities on the interface: application to a passenger ship. Comput Methods Appl Mech Eng. 198:3452–3463.
Naar H. 2006. Ultimate strength of hull girder for passenger ships [doctoral dissertation]. Espoo: Aalto University.
Okumoto Y, Takeda Y, Mano M, Okada T. 2009. Design of ship hull structures: a practical guide for engineers. Berlin/Heidelberg: Springer-Verlag.
Paulling JR, Payer HG, 1968. Hull-deckhouse interaction by finite element calculations. Annual Meeting of Society of Naval Architects and Marine Engineers. SNAME, New Jersey, NJ. p. 281–307.
Reddy JN, Ochoa OO. 1992. Finite element analysis of composite laminates. Dordrecht, The Netherlands: Kluwer Academic Publishers.
Romanoff J, Naar H, Varsta P. 2011. Interaction between web-core sandwich deck and hull girder of passenger ship. Mar Syst Ocean Technol. 6(1):39–45.
Romanoff J, Varsta P. 2007. Bending response of web-core sandwich plates. Compos Struct. 81:292–302.
Romanoff J, Varsta P, Remes H. 2007. Laser-welded web-core sandwich plates under patch-loading. Mar Struct. 20(1-2):25–48.
Satish Kumar YV, Mukhopadhyay M. 2000. Finite element analysis of ship structures using a new stiffened plate element. Appl Ocean Res. 22(6):361–374.
Whitney JM, Pagano NJ. 1970. Shear deformation in heterogenous anisotropic plates. J Appl Mech. 37(4):1031–1036.